International Journal of Bridge Engineering (IJBE), Vol. 13, No. 1, (2025), pp. 01-19

# NONLINEAR SIMULATION OF BRIDGE ABUTMENT-BACKFILL INTERACTION VIA HYPERBOLIC SPRINGS

Ali Vatanshenas

Doctor of Science (Technology), Alumnus of Tampere University, Tampere, Finland
e-mail: a.vatanshenas@gmail.com

**ABSTRACT:** This paper focuses on the nonlinear simulation of soil-wall interaction via a simple and efficient yet accurate solution. First, an overview of the subject and the reasoning behind using the proposed method is discussed. Then, the formulations are presented in a comprehensive and stepwise manner. At the end, a large-scale test found in the literature is studied and the precision of the method suggested in this research is verified via comparison between the force-displacement relationship between the simulation and the test program.

**KEYWORDS:** Abutment walls; Nonlinearity; Springs; Soil-structure interaction.

## 1 INTRODUCTION

### 1.1 General

This paper discusses part of the author's doctoral thesis on soil-structure interaction of bridges [1]. The subject presented in the following is focused on the wall-soil interaction under lateral loading considering soil nonlinear behaviour. One typical example of this kind is the bridge abutment wall pushed by the superstructure through the backfill. This phenomenon may occur even in isolated bridges where the superstructure can move freely towards the abutment wall and result in pounding if expansion joints are fully mobilized [2]. Figure 1 demonstrates a failure example of this kind, where the insufficient backfill resistance caused an increase of displacements and rotations in the wall which consequently amplified the moment and shear forces generated in the wall resulting in the failure of the wall and mobilizing the passive wedges in the backfill.

Soil is, indeed, a very complicated material with a high degree of uncertainty and variability, which makes its modelling a challenge for designers. Two modelling approaches are used when soil-structure interaction is involved, one focusing on the soil (i.e., continuum medium model) and another one prioritizing structure over the soil (i.e., spring model).

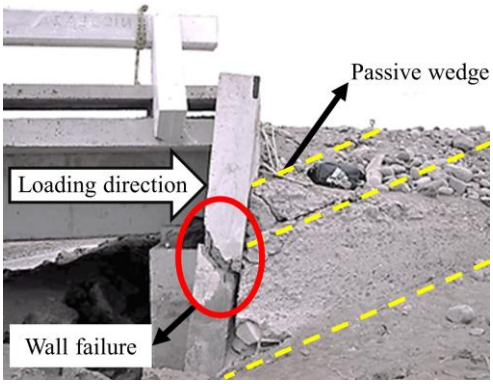


*Figure 1.* Abutment wall failure under horizontal loading and passive wedges mobilized behind the wall, modified from [3].

Figure 2 demonstrates an example of both approaches.

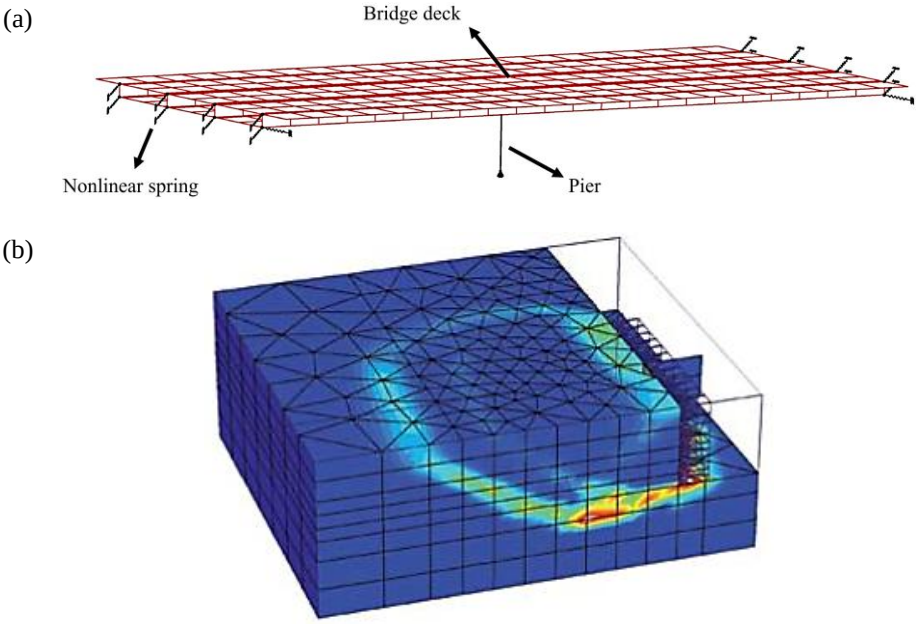


*Figure 2.* Abutment wall-backfill interaction approaches: a) spring model, modified from [4], and b) continuum medium model in Plaxis 3D [5].

## 1.2 Soil springs versus continuum modelling

Continuum models are indeed valuable and perhaps the best solution for understanding and simulation of materials in 6 dimensional degrees of freedom. However, soil continuum models are often quite complex and require many input parameters. Also, the high degree of uncertainty and variability in soil

makes the performance of constitutive soil models questionable. A good example emphasizing this issue is a deep excavation problem in Berlin sand which was analyzed by various analysts referred to as B1 to B17 from the university institutes and consulting companies recognized for numerical analysis in practical geotechnical engineering. Analysts were free to select their own soil model and make engineering judgments, if needed. The wall displacement estimation and selected soil model for each analyst are shown in Figure 3.

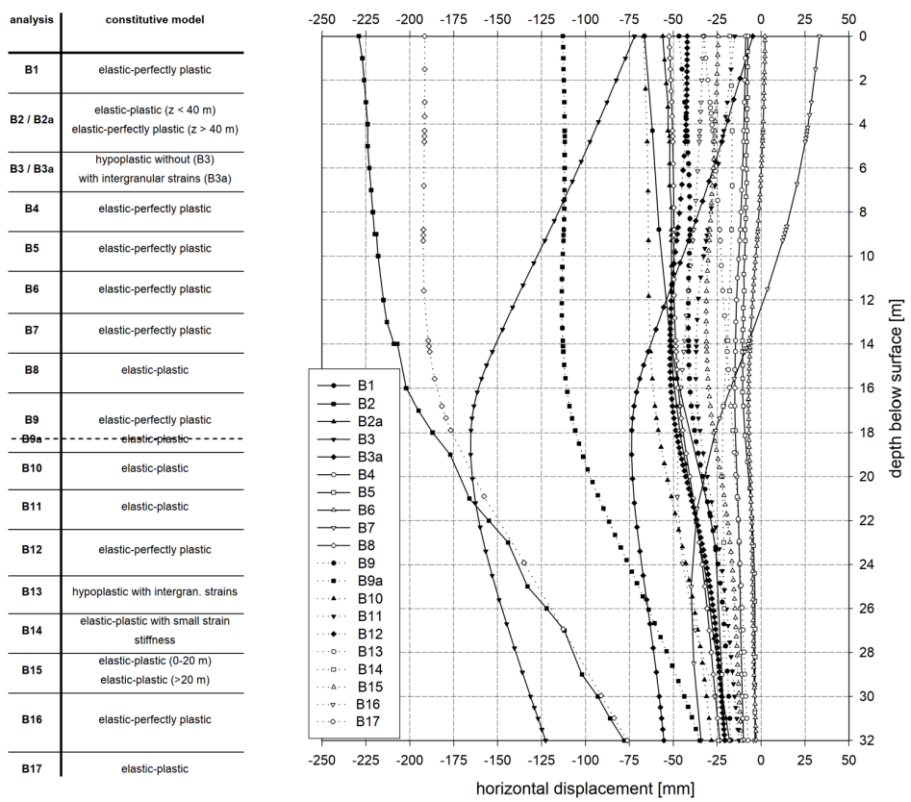


*Figure 3.* An example of continuum models application in practice: Estimation of final stage wall displacement computed by 17 analysts [6].

It is apparent that the scatter of the estimations is too high and, specifically, B2, B3, B3a, B9a, B7 and B17 are noticeably off the trend of results. After detailed evaluation of the results, Schweiger (2002) draws the conclusion that [6]:

***"We cannot neglect the user dependent scatter of 100%, since this is the reality in practice. The wide range of results submitted is by no means acceptable and unrealistic modelling assumptions may lead to consequences that the user of a particular code may not be aware of".***

Such estimation results highlight the importance of simple approaches like soil springs in practice that reduce misunderstanding and personal judgements.

## 1.3 Software limitations

Software packages are often aimed for structural (Abaqus, Ansys, etc.) or geotechnical (Plaxis, Flac, etc.) applications which cause problems when a detailed global model, including both soil and structural nonlinearity, is of interest. Some researchers tried to link multiple software packages via modular programming to benefit from the capabilities of various software packages, but this approach is quite complicated, inconsistent and time consuming. At the moment, due to software limitations, detailed modelling regarding one of the soil or structure has to be sacrificed, which presents the question that:

*Detailed modelling of which one is more logical for an SSI problem: Soil or structure?*

To answer this question, the author compares soil and structure based on the following factors: Input parameters, uncertainty and variability, and humans' life threat. The comparison between the soil and structure with respect to each factor is summarized below:

- **Input parameters:** Soil models are often formulated within the continuum mechanics platform and, as a result, they must obey some general rules such as hardening law, flow rule, etc. Continuum mechanics platform can become quite complex, for instance, when kinematic hardening or bounding surface models are used where multiple yield surfaces and hardening laws shall be defined.
- **Uncertainty and variability:** Soil is often a natural material, while structural materials like steel and concrete are man-made materials, and their characteristics like stiffness and strength can be set according to preference during the production phase. Therefore, it is fair to say that structural materials are, in general, more certain, and less variable, which is a beneficial aspect.
- **Humans' life threat:** Even though the soil and structure are often in interaction with each other, humans are in closer interaction with structures rather than the soil. The author believes the probability that a person gets injured during a catastrophic phenomenon (like earthquake, hurricane, flood, etc.) due to, for example, failure of a column is more than the probability of injury because of a soil wedge failure behind a retaining wall (structural elements are more vital elements). Moreover, during the past decades, in many parts of the world, the focus has been given only to the structures assuming the fixed base condition. However, these structures often tolerated severe loading conditions. In fact, in many cases, by considering soil effects a softer (longer fundamental period) numerical model is achieved which yields

to design with less force which would be a nonconservative but more economical approach.

All in all, it should be mentioned that choosing the level of complexity for SSI problems is case dependent. For instance, if a slope stability under multi directional dynamic loading is of interest, detailed 3D soil continuum modelling might be inevitable to capture real-like behaviour.

For the case of this study and the reasonings mentioned above, author thinks it would be more beneficial to focus on the "effects of soil behaviour" rather than "soil behaviour" itself. In other words, a simplified but more transparent modelling approach like spring models is prioritized over the complex solutions like constitutive soil models. Spring models are easy to develop in for instance spreadsheets and implement in software packages which makes them quite interesting for practical applications. All in all, "effects of soil behaviour" will be considered by using nonlinear springs in this study. The next sections discuss how to develop such springs and implement them in conjunction with structural elements to create and verify full nonlinear and efficient models suitable for practical applications.

# 2 THEORY

## 2.1 General

Passive earth pressure is required for obtaining $P_f$ of spring. There are various theories for computing passive earth pressure with different amounts of accuracy and complexity (Coulomb, Rankine, etc.). One study, [7] which covered a large-scale experiment indicated the acceptable performance of the Log Spiral method originated by Terzaghi [8]. As shown in Figure 4, the difference in these methods can be significant for computing the passive earth pressure. In the following, two relatively simple classical theories are mentioned briefly: Coulomb and Rankine. Underlying assumptions of these two models are listed in the following:

- Soil behaves homogenous and isotropic.
- Wall is considerably long, and soil layer extends in a long-distance (i.e., a semi-infinite condition exists).
- Soil is in drained condition.

Coulomb method is a very old approach that goes back to 1776 [10]. In this method, soil failure is assumed to be planar as a translation of a rigid body. The passive earth pressure per length is obtained by using the following relation:

$$E_p = \frac{1}{2} K_p \gamma H^2 \tag{1}$$

Where $K_p$ is the coefficient of passive earth pressure, $\gamma$ is the unit weight of soil, and $H$ is the height of the wall. Furthermore, the failure force $P_f$ is obtained from the equation below:

$$P_f = E_p WR = \frac{1}{2} K_p \gamma H^2 WR \tag{2}$$

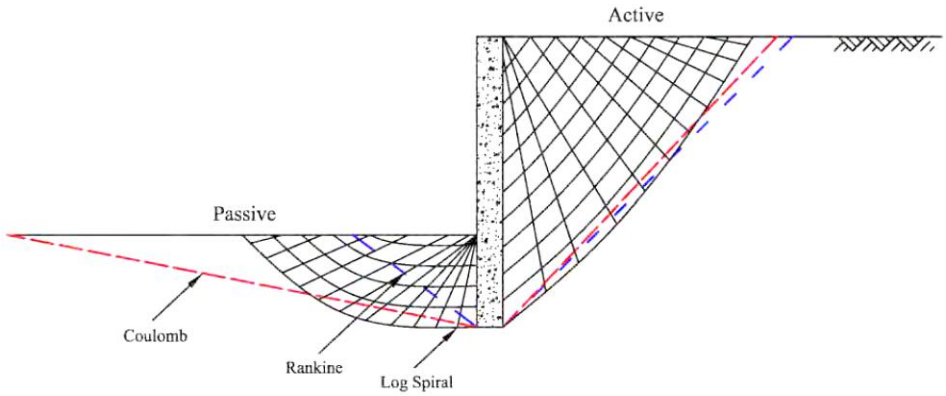


*Figure 4.* Difference in failure trends, using Coulomb, Rankine, and Log Spiral methods [9].

Where, $W$ is the width of the wall, and $R$ is called the 3D shape modification factor. Traditional earth pressure theories only take into account the 2D state, which assumes a significantly long wall moving towards the soil. Therefore, for short walls (also pile caps), wider passive wedges occur due to the 3D condition (Figure 5a). Ovesen (1964) proposed an equation to compute $R$ [11]:

$$R = 1 + (K_p - K_a)^{2/3} \left[ 1.1(1 - \frac{H}{z+H})^4 + \frac{1.6B}{1+5\frac{W}{H}} + \frac{0.4(K_p - K_a)(1-\frac{H}{z+H})^3 B^2}{1+0.05\frac{W}{H}} \right] \tag{3}$$

Where, $K_a$ is the coefficient of active earth pressure, $B$ is a factor considering the spacing effect where multiple walls or pile caps exist close to each other ($B$=1 when only one wall is present), and $z$ is the embedment depth of the wall beneath the soil surface. Mokwa and Duncan (2002) suggest $R \approx 2$ as a convenient and conservative value for abutment walls [12]. A schematic of forces acting on a wall in out of the plane direction is given in Figure 5b.
Also, $K_p$ is obtained by using the equation below:

$$K_p = \frac{sin^2(\alpha - \Phi')}{sin^2(\alpha) sin(\alpha+\delta)[1 - \sqrt{\frac{sin(\Phi'+\delta) sin(\Phi'+\beta)}{sin(\alpha+\delta) sin(\alpha+\beta)}}]^2} \tag{4}$$

Where $\beta$ is the angle between a horizontal line and ground surface, $\Phi'$ is the drained friction angle of the soil, $\alpha$ is the angle between a horizontal line and back face of the wall, and $\delta$ is the angle of wall friction. By assuming $\alpha$=90, $\beta$=0, and $\delta$=0, the equation above simplifies to the well-known equation:

$$K_p = \frac{1+sin(\Phi')}{1-sin(\Phi')} = tan^2(45 + \frac{\Phi'}{2}) \tag{5}$$

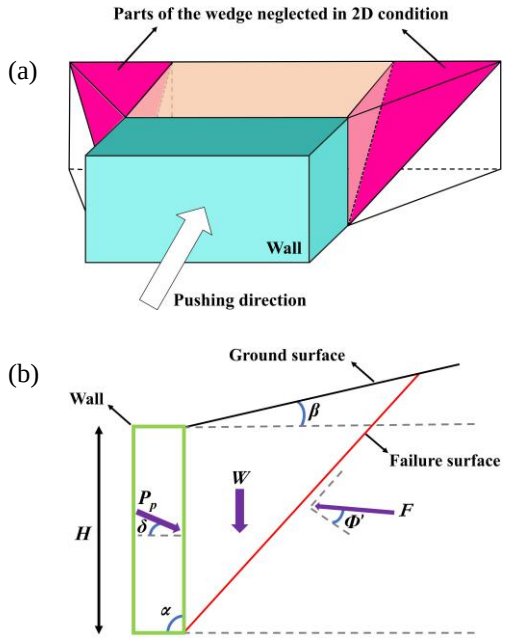


*Figure 5.* Passive wedge presentation: a) 3D view, and b) 2D view including the forces acting on a wall [1].

The Coulomb method takes the wall friction into account. Nevertheless, it assumes a planar failure surface. Consequently, $K_p$ values are obtained unrealistically high when $\delta > 0.5\Phi'$ [13].

## 2.2 Hyperbolic springs

Soil behaviour can be approximated using hyperbolic functions [14]. For instance, Duncan and Chang (1970) proposed a hyperbolic relation between the deviatoric stress $q$, and axial strain, $\varepsilon$ [15]:

$$q_i = \frac{\varepsilon_i}{\frac{1}{E_{max}} + \frac{\varepsilon_i}{q_{ult}}} \tag{6}$$

Where, $E_{max}$ and $q_{ult}$ are the initial elastic modulus, and ultimum deviatoric stress, respectively. By assuming isotropic linear elasticity, $E_{max}$ could be related to the maximum shear modulus, $G_0$ and Poisson's ratio, $\nu$ through:

$$E_{max} = 2G_0(1+\nu) \tag{7}$$

Indicating the failure point based on the Equation (6) is uncertain since the stress-strain curve does not always reach an asymptotic line in large strains. Therefore, a new quantity named stress level, SL was introduced where SL=1 represents the fully mobilized stress condition (i.e., failure point):

$$SL = \frac{q_i}{q_{ult}} \tag{8}$$

Figure 6 clarifies the parameters used for estimating nonlinear soil behaviour. To utilize failure deviatoric stress, $q_f$, instead of the uncertain $q_{ult}$ in the hyperbolic equation, failure ratio, $R_f$ is used, which is simply obtained by the following relation:

$$R_f = \frac{q_f}{q_{ult}} \tag{9}$$

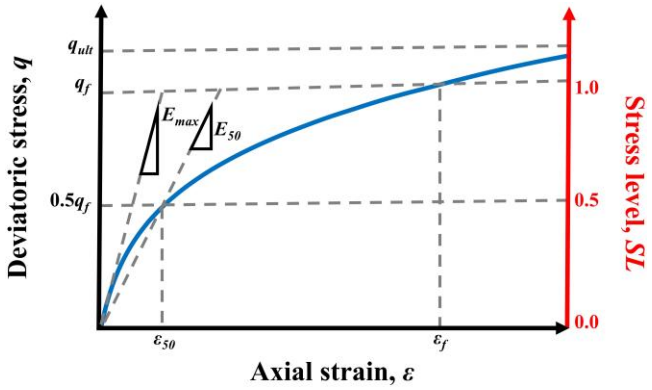


*Figure 6.* Nonlinear stress-strain relationship [1]

As shown in Figure 6, $q_f$ is quite close to $q_{ult}$. One study pointed out lower and upper limits of $R_f$: $0.94 \leq R_f \leq 0.98$ and, suggested $R_f$=0.97 as a good estimate [3]. By multiplying Equation (6) into $R_f$ /$R_f$ the following hyperbolic relation is obtained which is now dependent on $q_f$ and not directly to the $q_{ult}$:

$$q_i = \frac{\varepsilon_i}{\frac{1}{E_{max}} + \frac{\varepsilon_i R_f}{q_f}} \tag{10}$$

By exploiting the equation above, the stress level given in Equation (8) can also be computed by the following relation:

$$SL = \frac{\varepsilon_i}{\frac{q_f}{E_{max}} + \varepsilon_i R_f} \tag{11}$$

Nevertheless, measuring $E_{max}$ is not straightforward, and its value is highly affected by many parameters like soil disturbance, confinement pressure, stress history, etc. Consequently, the obtained relation for $q_f$ was not user friendly. Later, to reach a more practical approach, the hyperbolic relation was rearranged to ease the parameter acquisition by using ordinary tests [16]:

$$q_i = \frac{\varepsilon_i}{\frac{\varepsilon_f \varepsilon_{50}}{\varepsilon_f - \varepsilon_{50}} + \left(\frac{\varepsilon_f - 2\varepsilon_{50}}{\varepsilon_f - \varepsilon_{50}}\right)\varepsilon_i} \left(\frac{q_f}{R_f}\right) \tag{12}$$

Where the first term represents SL and the second term $q_{ult}$ in the equation above. $\varepsilon_{50}$ values are reported for different soil types (Table 1). In addition, $\varepsilon_f$ is reported as being 31 times larger than $\varepsilon_{50}$ based on 144 triaxial tests [17].

*Table 1.* Approximated values of $\varepsilon_{50}$ [17]

| **Dominant soil type** | $\varepsilon_{50}$ | |
|---|---|---|
| | **value range** | **Approximated value** |
| Gravel | 0.001-0.005 | 0.0035 |
| Clean sand (0-12% Fine grains) | 0.002-0.003 | 0.0035 |
| Silty sand (12-50% Fine grains) | 0.003-0.005 | 0.0035 |
| Silt | 0.005-0.007 | 0.007 |
| Clay | 0.0075 | 0.007 |

However, to model soil as spring element, "force-displacement" relationship is required not "stress-strain". The hyperbolic force-displacement relationship proposed by Duncan and Mokwa (2001) keeps the same format as Equation (10), but with different parameters [13]:

$$p_i = \frac{y_i}{\frac{1}{K_{max}} + \frac{y_i R_f}{P_f}} \tag{13}$$

Where $p$ is the lateral force, and $y$ is the lateral displacement. $K_{max}$ is the initial stiffness approximated by utilizing the elastic response of a horizontal load on a vertical rectangle which requires $E_{max}$ and Poisson's ratio, $v$ for its computation [18]. It is fair to say that similar to $E_{max}$, computing $K_{max}$ is not straightforward. Alternatively, approximated values of $K_{max}$ for granular materials are reported by Cole and Rollins (2006) based on the work of Douglas and Davis (1964) in Table 2 [19].

*Table 2.* Elasticity parameters for granular soil types [19]

| **Soil type** | $D_r$**(%)** | $E_{max}$**(Mpa)** | $v$ | $K_{max}$**(kN/m)** |
|---|---|---|---|---|
| Clean sand | 63 | 37.1 | 0.27 | 246000 |
| Fine gravel | 54 | 33.8 | 0.31 | 226000 |
| Coarse gravel | 69 | 39.0 | 0.26 | 259000 |
| Silty sand | 67 | 38.3 | 0.35 | 260000 |

$R_f$ is the force failure ratio (here $R_f$=$P_f$ /$P_{ult}$) reported to be in the range of $0.75 \leq R_f \leq 0.95$ by [13], and $P_f$ is the failure force computed from the passive earth pressure theories (i.e., Coulomb, Rankine, Log Spiral, etc.). Similar to the Figure 6, force-displacement parameters are illustrated graphically in Figure 7.

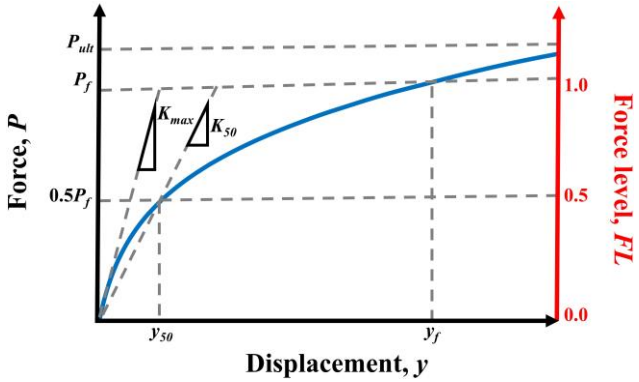


*Figure 7.* Nonlinear force-displacement relationship [1].

# 3 CASE STUDY

## 3.1 Case description

The considered case in this section is a large-scale test conducted by the structural and geotechnical engineering laboratory of the University of California, Los Angeles (UCLA). In this experiment, a reinforced concrete wall with dimensions of $4.572m \times 2.5908m \times 0.9144m$ is pushed horizontally into the compacted silty sand backfill placed behind the wall. Wall section details were not available.

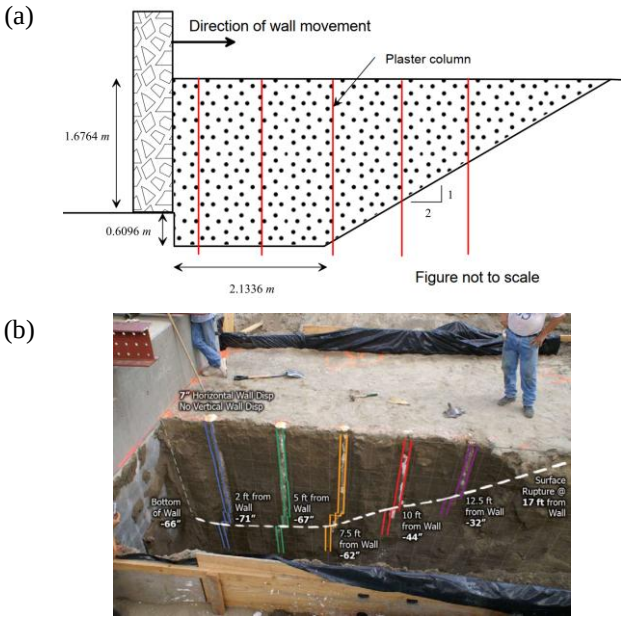


*Figure 8.* Schematic of the experiment: a) dimensions, and b) failure surface after the test, modified from [7].

However, Professor Stewart informed the author that the wall remained elastic after the test. Gypsum columns were also drilled into the backfill to investigate the failure surface trend after the test. The results of this interesting research are implemented into the Caltrans code of practice, Caltrans (2019) as well [20]. Further details regarding the test procedure are referred to [7,21]. Geometry and the actual schematic of the test are shown in Figure 8.

The concrete used in the wall has a density of $22.77 kN/m^3$ with average compressive strength and an average modulus of elasticity of $39989.6 kN/m^2$ and $26659682.22\ kN/m^2$, respectively. Also, the angle of wall friction is reported to be $\delta$=14°. The backfill has a dry density of $19.95 kN/m^3$, and a friction angle of 40°.

## 3.2 Modelling

First, at-rest or even active earth pressure might need to be considered before simulating the backfill in passive condition. A straightforward approach is assigning the at-rest or active earth pressure as a preload to the wall. Then, the wall can be simulated in passive condition using nonlinear springs.

In the following, soil nonlinear spring is defined by using Equation (13) proposed by [13] where failure ratio $R_f$ is assumed to be 0.97 and the passive earth pressure coefficient is obtained from the coulomb method ($K_p$=8.44). This value is quite close to the $K_p$ reported in the test report, using the more accurate Log Spiral method ($K_p$=7.95). Also, $K_{max}$ is obtained from Table 2, where $K_{max}$=260000*kN/m* for silty sand soil. Failure force is also computed by the Coulomb method, $P_f$=2159.78*kN*. All of the parameters used for defining the nonlinear soil spring are summarized in Table 3.

*Table 3.* Required parameters for modelling soil nonlinear spring.

| Parameter | Symbol | Unit | Value |
|---|---|---|---|
| Backfill friction angle | $\Phi'$ | *deg* | 40 |
| Angle between a horizontal line and ground surface | $\beta$ | *deg* | 0 |
| Angle between a horizontal line and back face of the wall | $\alpha$ | *deg* | 90 |
| Angle of wall friction | $\delta$ | *deg* | 14 |
| Unit weight of backfill | $\gamma$ | $kN/m^3$ | 19.95 |
| Height of the wall | $H$ | *m* | 1.6764 |
| Width of the wall | $W$ | *m* | 4.5720 |
| Failure ratio | $R_f$ | - | 0.97 |
| 3D modification factor | $R$ | - | 2 |
| Initial stiffness | $K_{max}$ | *kN/m* | 260000 |

Three models are created for simulating wall-backfill interaction. Choosing the appropriate model is dependent on the amount of accuracy and the type of required outputs. In the following, each model is described.

### *3.2.1 Model 1 (1 spring)*

In this model, only one multilinear plastic spring is defined based on Equation (13) and parameters listed in Table 3. This model is the simplest when compared to the others. It only produces a force-displacement relationship and the wall itself is not modelled. However, it can be a convenient and fast approach for a preliminary analysis or simplified models like spline bridges where the deck is modelled by using frame elements.

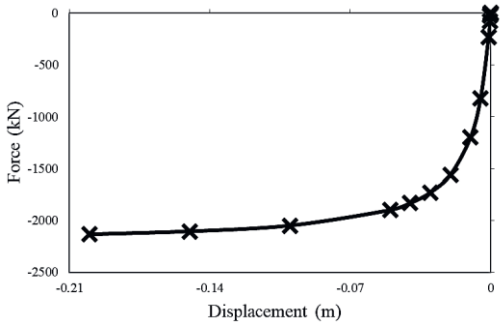


*Figure 9.* Simulating the wall-backfill interaction using one spring [1].

### *3.2.2 Model 2*

In this model, the spring defined in Model 1 (1 Spring) is divided into 11 springs distributed along the depth of the soil layer with an interval of 0.1524*m*. Also, the wall is modelled using frame element (Figure 10).

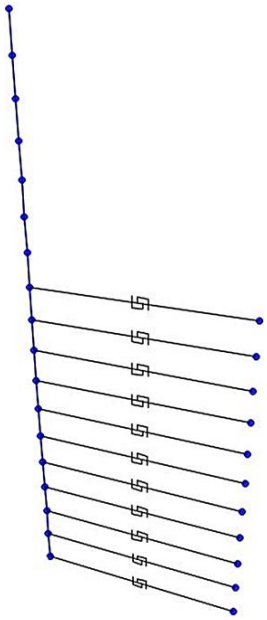

*Figure 10.* Eleven springs distributed along the depth of the soil layer [1]

To define the force-displacement relationship for each spring, consider the linear distribution trend given in Figure 11.

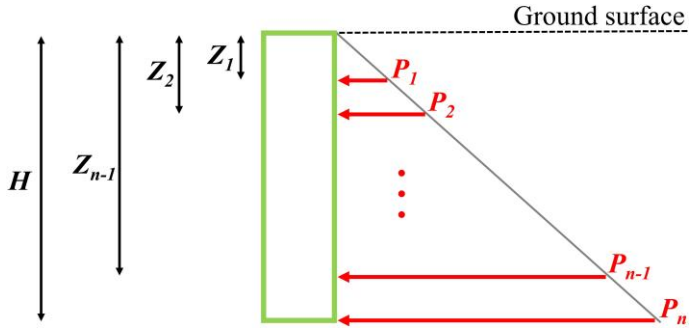


*Figure 11.* Linear distribution of forces along the depth [1]

Based on trigonometry, the following relations are observed between the forces:

$$\frac{P_1}{Z_1} = \frac{P_2}{Z_2} = \cdots = \frac{P_{n-1}}{Z_{n-1}} = \frac{P_n}{H} \tag{14}$$

The above relation can be rearranged to obtain the following equation:

$$P_i = P_n \frac{Z_i}{H} \quad , i = 1, 2, \ldots, n\text{-}1, n \tag{15}$$

Also, a summation of distributed forces should equal the failure force $P_f$ as defined in Model 1 (1 Spring):

$$\sum_1^n P_i = \frac{P_n}{H} \sum_1^n Z_i = P_f \tag{16}$$

Therefore, the failure force for the last spring $P_n$ is achieved as:

$$P_n = \frac{P_f H}{\sum_1^n Z_i} \tag{17}$$

Consequently, by knowing $P_n$ and spring intervals $Z_i$ other forces are obtained by using Equation (15). Similarly, the following relations exist for the stiffness:

$$K_i = K_n \frac{Z_i}{H} \quad , i = 1, 2, \ldots, n\text{-}1, n \tag{18}$$

$$K_n = \frac{K_{max} H}{\sum_1^n Z_i} \tag{19}$$

All in all, the hyperbolic relation for the $i^{th}$ spring is obtained as:

$$p_i = \frac{y_i}{\frac{1}{K_n \frac{Z_i}{H}} + \frac{y_i R_f}{P_n \frac{Z_i}{H}}} \tag{20}$$

Finally, multilinear plastic springs defined for Model 2 are plotted in Figure 12.

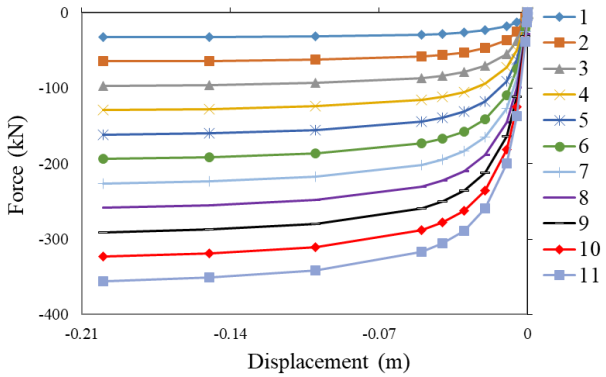


*Figure 12.* Nonlinear springs distributed along the depth of the wall in Model 2 [1]

### *3.2.3 Model 3*

In this model, the 11 springs in Model 2 are distributed along the width of the wall. In total, 341 springs are assigned to the wall. Note that springs at the edge represent the effect of less portion of the soil. Therefore, two sets of springs are defined for the middle and edge zones for each elevation by multiplying the Equation (20) into a distribution factor:

$$p_{i-Middle} = \frac{y_i}{\frac{1}{K_n \frac{Z_i}{H}} + \frac{y_i R_f}{P_n \frac{Z_i}{H}}} \left(\frac{1}{(n_t-2)+1}\right) \tag{21}$$

$$p_{i-Edge} = \frac{P_{i-Middle}}{2} \tag{22}$$

Where $n_t$ is the total number of nodes in one elevation (here $n_t$=31). Soil springs defined for Model 3 are shown in Figure 13.

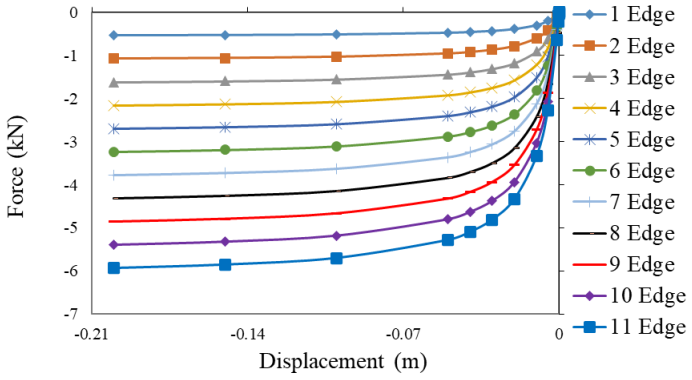


(a)

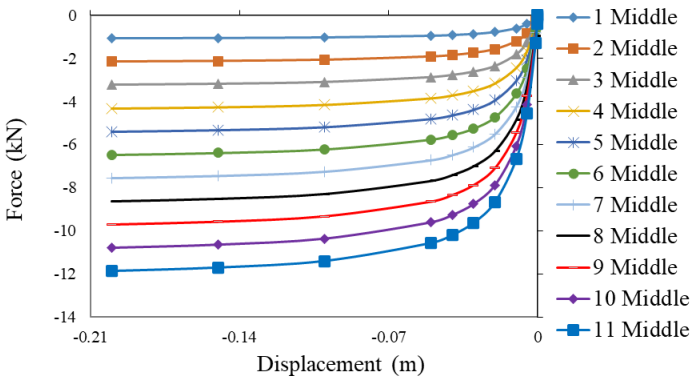


(b)

*Figure 13.* Nonlinear springs used in Model 3: a) edge springs, and b) middle springs [1]

In addition, the wall is modelled by using a plate element consisting of 510 mesh elements with equal dimensions of $0.1524m \times 0.1524m$. Figure 14 demonstrates Model 3.

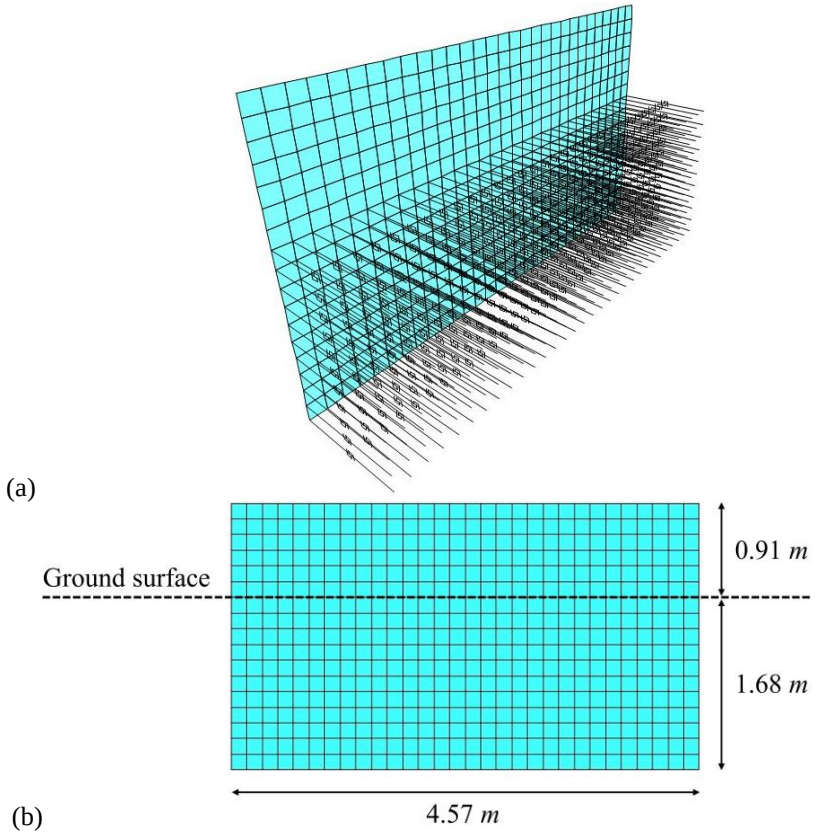


*Figure 14.* Model 3: a) 3D view, and b) 2D view including the dimensions [1]

Here it is worth mentioning that the stress generated at the edges and corners might not be the exact value. One alternative to the approach used here would be distributing the springs along the wall with various multipliers. Such an approach has been previously suggested for footing-half space soil problems. For instance, two studies present variant distribution of soil springs in order to consider the non-uniform stress distribution under a rigid foundation on elastic half space. Bellmann and Katz (1994) suggest four times increase in the stiffness of soil where only one row of springs beside the edges are multiplied by a factor of four [22]. Also, Dörken and Dehne (2007) recommend a linear increase of stiffness at the quarter distance of the wall close to the edges [23]. Figure 15 demonstrates these two methods.

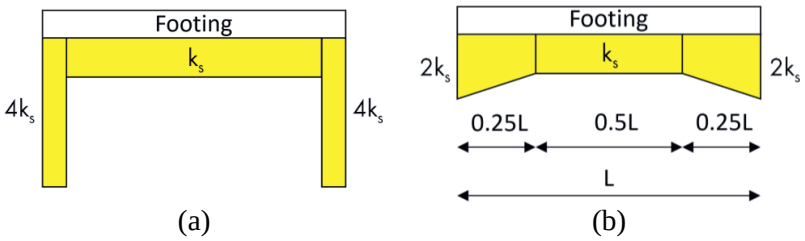


*Figure 15.* Stiffness distribution based on a) Bellmann and Katz (1994) [22], and b) Dörken and Dehne (2007) [23]

Also, for the case of bridges where often abutment wall-wing walls-backfill interaction is of interest (i.e., U-shaped wall), the estimation of stress will be even more complex compared to a single wall-backfill case. However, , in terms of the ”force-displacement" relationship, the proposed distribution of springs in this study works well enough for practical purposes.

## 4 RESULTS

A Nonlinear static (pushover) analysis is performed. In this type of analysis, the response of the model is recorded step by step as the loading increases.
In addition to models’ estimation and test results, three other graphs are given for comparison:

1. An equation proposed by [3]:

$$p_i = \frac{y_i}{0.011 + 0.03y_i} \quad \text{(for granular backfill. } y \text{ in inches, } p \text{ in } Kips/ft \text{ of wall)} \quad (23)$$

2. A bilinear graph based on [20]. In this graph, the force and stiffness are computed via:

$$P_{f-Caltrans} = W\left(\frac{5.5H^{2.5}}{1+2.37H}\right)R_{skew} \quad (W \text{ and } H \text{ are in inches, } P \text{ in } Kips) \quad (24)$$

$$K_{Caltrans} = W(5.5H + 20)R_{skew} \quad (W \text{ and } H \text{ are in inches, } K \text{ in } Kips/in) \quad (25)$$

As illustrated in Figure 16, $R_{skew}$ is a modification factor taking effects of skew angle, $\theta$ into account via evaluating large scale tests conducted by [24]:

$$R_{skew} = e^{-\theta/45} \tag{26}$$

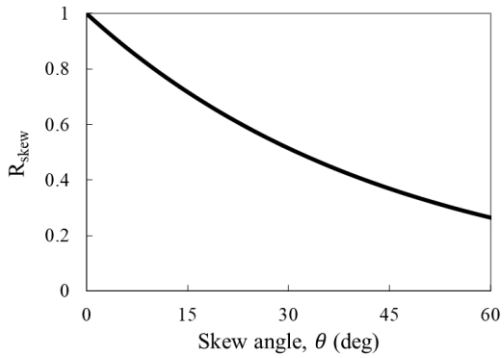


*Figure 16.* $R_{skew}$ values recommended by [20], after [24]

3. An idealized bilinear graph assuming following constraints:
   - The idealized graph should reach $P_f$ in large strains
   - The area beneath the hyperbolic models and the bilinear graph should be the same

Exploiting the assumptions above, the yield displacement $y_{eff}$ and effective stiffness $K_{eff}$ of the idealized graph are obtained as:

$$y_{eff} = 2y_f - \frac{2\,(Area\ beneath\ the\ hyperbola)}{P_f} \tag{27}$$

$$K_{eff} = \frac{P_f}{y_{eff}} \tag{28}$$

As illustrated in Figure 17, a comparison of models with the test result shows good agreement, especially in lower stress levels.

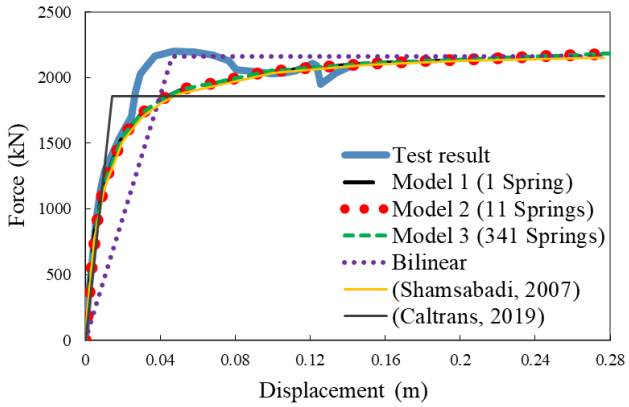


*Figure 17. Comparison between test result and models' performance* [1]

Note that all three models created in this study follow the same path since they represent the same behaviour in terms of force-displacement, but they differ in terms of output types. For instance, the simple Model 1 (1 Spring) does not produce additional output and only the force-displacement curve.

In addition, Shamsabadi's equation which is only valid for a special backfill material gives almost identical results compared to the models created in this study. However, in the bilinear plots, stiffness is not obtained realistically and in the case of [20], the failure force is estimated less than other models.

## 5 CONCLUSIONS

First, a general discussion about the importance of the subject was given in a logical way. Then, theory and formulation of wall-soil interaction was presented thoroughly in a stepwise and coherent manner. Next, application of the proposed method was covered via studying a real-life wall-backfill interaction example. Various modelling techniques were also discussed in detail. Finally, the verification of the methods and assumptions were checked through comparison of the nonlinear analysis with test data.

## REFERENCES

[1] Vatanshenas A. Nonlinear Soil-structure Interaction of Bridges: Practical Approach Considering Small Strain Behaviour. *Doctoral Thesis, Tampere University*. 2024. ISBN: 978-952-03-3234-1.

[2] Vatanshenas A, Rohanimanesh MS, Mohammadiha E. Investigating the Performance of Viscoelastic Dampers (VED) Under Nearfield Earthquakes with Directivity Feature. Civil and Environmental Engineering. 2018d Jun 1;14(1):21-7.

[3] Shamsabadi A. Three-dimensional nonlinear seismic soil-abutment-foundation-structure interaction analysis of skewed bridges. University of Southern California; 2007.

[4] Shamsabadi A, Kapuskar M. Nonlinear soil–abutment–foundation–structure interaction analysis of skewed bridges subjected to near-field ground motions. Transportation research record. 2010;2202(1):192-205.

[5] Shamsabadi A, Nordal S. Modeling passive earth pressures on bridge abutments for nonlinear seismic soil-structure interaction using Plaxis. Plaxis Bulletin. 2006 Oct;20:8-15.

[6] Schweiger HF. Benchmarking in geotechnics 1. Computational Geotechnics Group. CGG IR006. 2002 Mar.

[7] Stewart JP, Taciroglu E, Wallace JW, Ahlberg ER, Lemnitzer A, Rha C, Tehrani P, Keowen S, Nigbor RL, Salamanca A. Full scale cyclic testing of foundation support systems for highway bridges. Part II: Abutment backwalls. 2007.

[8] Terzaghi K. Theoretical soil mechanics. johnwiley & sons. New York. 1943:11-5.

[9] Shamsabadi A, Xu SY, Taciroglu E. Development of Improved Guidelines for Analysis and Design of Earth Retaining Structures. University of California, Los Angeles (UCLA), Structural and Geotechnical Engineering Laboratory, UCLA-SGEL Report. 2013a Jul;2:243.

[10] Coulomb, CA. Essai sur une application des regles des maximis et minimis a quelques problemes des statique relatifs a l'architecture. Mem. Acad. Des Sciences. 1776; Paris, France.

[11] Ovesen NK. Anchor slabs, calculation methods and model tests. Bulletin. 1964;16:39.

[12] Mokwa RL, Duncan JM. Investigation of the resistance of pile caps and integral abutments to lateral loading. Virginia Center for Transportation Innovation and Research; 2002 Feb 1.

[13] Duncan JM, Mokwa RL. Passive earth pressures: theories and tests. Journal of Geotechnical and Geoenvironmental Engineering. 2001 Mar;127(3):248-57.
[14] Kondner RL. Hyperbolic stress-strain response: cohesive soils. Journal of the Soil Mechanics and Foundations Division. 1963 Feb;89(1):115-43.
[15] Duncan JM, Chang CY. Nonlinear analysis of stress and strain in soils. Journal of the soil mechanics and foundations division. 1970 Sep;96(5):1629-53.
[16] Schanz T, Vermeer PA, Bonnier PG. The hardening soil model: formulation and verification. Beyond 2000 in computational geotechnics. 1999 Jun:281-96.
[17] Norris GM. Theoretically based BEF laterally loaded pile analysis. In Proceedings of the 3rd international conference on numerical methods in offshore piling 1986 May (pp. 361-386). Navtes.
[18] Douglas DJ, Davis EH. The movement of buried footings due to moment and horizontal load and the movement of anchor plates. Geotechnique. 1964 Jun;14(2):115-32.
[19] Cole RT, Rollins KM. Passive earth pressure mobilization during cyclic loading. Journal of Geotechnical and Geoenvironmental Engineering. 2006 Sep;132(9):1154-64.
[20] SEISMIC DESIGN CRITERIA VERSION 2.0. State of California Department of Transportation. 2019.
[21] Stewart JP, Taciroglu E, Wallace JW, Lemnitzer A, Hilson CH, Nojoumi A, Keowan S, Nigbor RL, Salamanca A. Nonlinear load-deflection behavior of abutment backwalls with varying height and soil density. California. Dept. of Transportation. Division of Research and Innovation; 2011 Dec 1.
[22] Bellmann J, Katz C. Bauwerk-Boden-Wechselwirkungen, 3. FEM/CAD-Tagung Darmstadt, TH Darmstadt. 1994.
[23] Dörken W, Dehne E. Grundbau in Beispielen Teil 2–Kippen, Gleiten, Grundbruch, Setzungen, Flächengründungen, Stützkonstruktionen, Vergleich mit dem alten Sicherheitskonzept; Risse im Bauwerk.
[24] Shamsabadi A, Rollins KM. Three-dimensional nonlinear continuum seismic soilstructure interaction analysis of skewed bridge abutments. InProcs., 8th European Conf. on Numerical Methods in Geotechnical Engineering, Delft, the Netherlands 2014.